ECS Transactions, 35 (1) 1161-1169 (2011)
10.1149/1.3570099 ©The Electrochemical Society

Influence of Small Amounts of NiO on the Electrical Conductivity of 8YSZ

R. M. Batista and E. N. S. Muccillo

Energy and Nuclear Research Institute-CCTM, S. Paulo 05508-000, SP, Brazil

The effect of small amounts of nickel oxide on the microstructure and the electrical conductivity of zirconia-8 mol% yttria was systematically investigated by scanning electron microscopy and impedance spectroscopy techniques. Nickel carbonate was added to commercial yttria-stabilized zirconia powder, and the mixture was used to prepare green compacts. Sintering experiments were carried out at several sintering temperatures. The electrical conductivity of sintered specimens are similar for nickel oxide additions up to 1 mol% and sintering times up to 5 h. For larger sintering times, reduction of the grain boundary electrical conductivity, along with microstructure defects were observed in specimens containing the additive. Energy-dispersive spectroscopy analysis in several micro-regions of sintered specimens revealed a heterogeneous distribution of nickel. The nickel segregation phenomenon occurring with long sintering times is responsible for an additional blocking effect on the electrical conductivity of the solid electrolyte.

Introduction

Many investigations in the field of solid oxide fuel cells have focused on the development of new materials for this type of application, but yttria-stabilized zirconia (YSZ), the cermet Ni/YSZ, and lanthanum strontium manganite (LSM) are still the most used materials for solid electrolyte, anode and cathode, respectively (1).

This application requires a high density solid electrolyte in order to be impervious to the diffusion of molecular oxygen. Commercial 8 mol% yttria-stabilized zirconia (8YSZ) powder attains such high density after conventional sintering only at temperatures higher than 1350ºC (2). The decrease of the sintering temperature to around 1200ºC could allow for simultaneous sintering of the solid electrolyte and the anode components. This has been one of the pursued targets over the last years, important in reduction of manufacturing costs of this type of device.

One approach to lower the sintering temperature of ceramic materials is by the use of sintering aids. Previous works have demonstrated the effectiveness of sintering additives in the densification of yttria-stabilized zirconia, especially those based on transition metals (3-6). The relatively low melting temperature of the transition metal-based additives allows for densification of the specimens under study by a liquid phase mechanism. Nickel oxide, NiO, has a cubic crystalline structure and relatively high melting point (1984ºC) (7). There are relatively few studies related to the addition of this metal oxide to yttria-stabilized zirconia.

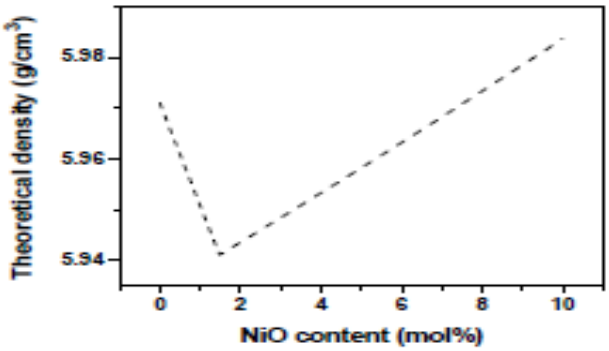

Figure 1. Evolution of the theoretical density of 8YSZ with NiO content.

The theoretical density of 8YSZ decreases up to ~ 1.5 mol% of the additive and then increases. This decrease is attributed to the relatively lower mass of Ni compared to Y and Zr and reveals that NiO is incorporated into solid solution up to 1.5 mol%, approximately.

The linear shrinkage increases with increasing the content of NiO. Figure 2 shows the variation of the temperature for maximum shrinkage, T_{MAX}, with nickel oxide content.

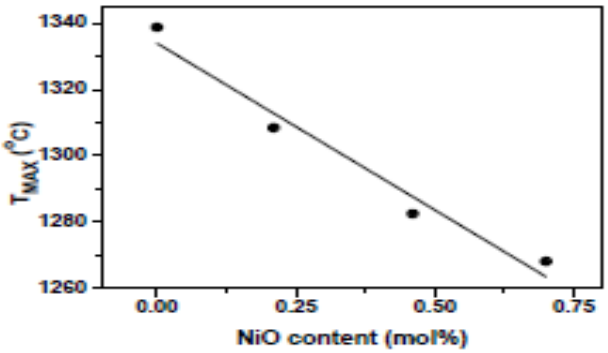

Figure 2. Variation of the temperature of maximum shrinkage with NiO content.

This result shows that NiO addition in contents lower than 1 mol% allows for reducing the dwell temperature of 8YSZ by about 60°C.

Densification was also investigated by apparent density measurements for longer (15 h) sintering times. Figure 3 shows the variation of the apparent density with the dwell temperature for specimens containing up to 1 mol% NiO.

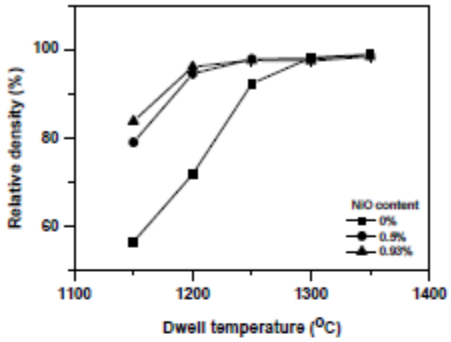

Figure 3. Relative density of specimens with varying NiO contents as a function of the dwell temperature. Sintering time = 15 h.

The relative density of specimens containing NiO is higher than that of pure 8YSZ below 1300ºC. For a NiO content of only 0.5 mol%, the relative density is about 94.6% at 1200ºC, whereas that of pure 8YSZ is 72%. Above 1300ºC, the relative density of all specimens has similar values.

Figure 4 shows scanning electron microscopy (SEM) micrographs of fractured surfaces of (a) 8YSZ and (b) 8YSZ with 0.5 mol% of NiO.

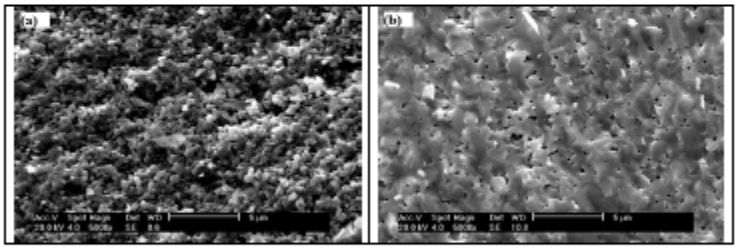

Figure 4. SEM micrographs of (a) pure 8YSZ and (b) 8YSZ with 0.5 mol% NiO specimens sintered at 1350ºC for 0.1 h.

The specimen containing NiO (figure 4b) shows low porosity compared to pure 8YSZ (figure 4a). The preferential mode of fracture is transgranular. SEM observations in polished and thermally etched surfaces revealed that NiO addition to 8YSZ enhances the grain growth process. The evolution of the grain size in specimens sintered at several soaking times at 1350ºC with varying NiO contents is shown in figure 5. The increase in the mean grain size with soaking time and NiO content, especially up to 1 mol% of the additive, is remarkable. For nickel oxide contents above the solubility limit, the grain size attains a steady state.

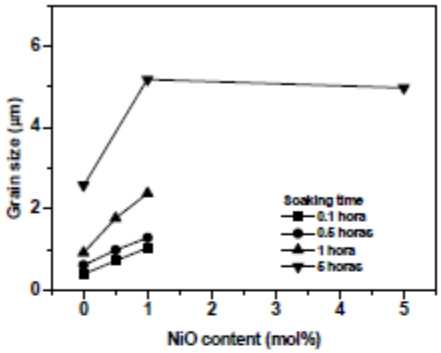

Figure 5. Evolution of the grain size of 8YSZ with sintering time at 1350ºC and for varying NiO contents.

Figure 6 shows impedance spectroscopy diagrams of 8YSZ specimens containing 0-1.0 mol% NiO. The temperature of measurement is indicated for each diagram.

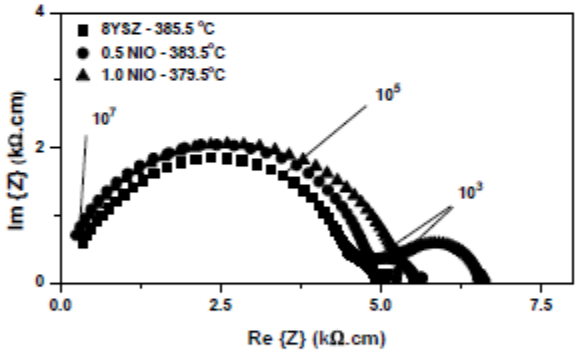

Figure 6. Impedance spectroscopy diagrams of 8YSZ specimens containing 0-1 mol% NiO. Numbers are the relaxation frequency (in Hz).

Two well-resolved semicircles are seen in all these plots related to the grain (high frequency) resistivity and to the blocking effect at grain boundaries (low frequency). The diameter of the grain boundary semicircle increases with increasing the nickel oxide content, mainly above the solubility limit, as expected. The Arrhenius plots of the grain conductivity for 8YSZ (a) and 8YSZ with 1.0 mol% nickel oxide (b) are shown in figure 7. These plots of grain conductivity show that the mechanism for electrical conduction is similar for all studied specimens. The apparent activation energy for grain conductivity calculated from the slopes of these plots is similar: 1.10 (8YSZ) and 1.14 eV (1.0 mol % NiO specimens).

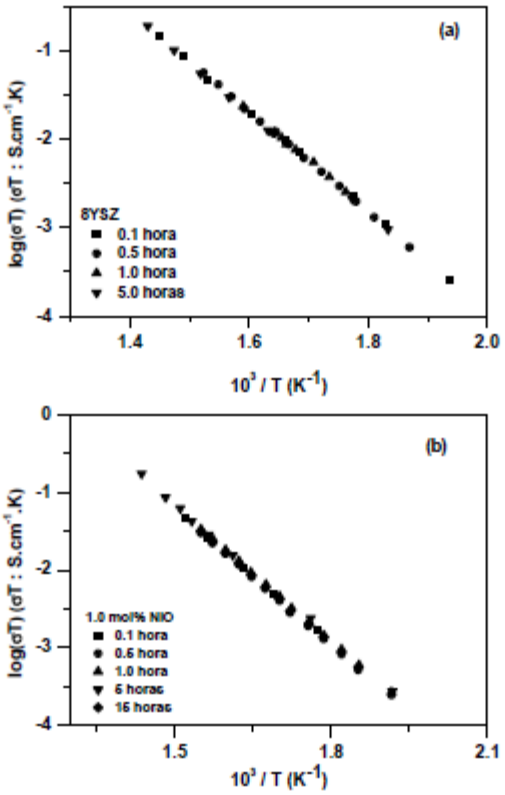

Figure 7. Arrhenius plots of the grain conductivity for (a) 8YSZ and (b) 8YSZ containing 1.0 mol% NiO sintered at 1350ºC for varying sintering times.

The grain boundary blocking effect of 8YSZ is known to decrease with increasing sintering time due to decrease in the grain boundary density (number of grain boundaries per unit length). Similar effect occurs for specimens containing nickel oxide except for those sintered for larger sintering times (figure 8). It is worth noting the decrease in the grain boundary conductivity after 15 h of sintering time. The calculated apparent activation energy is 1.17 ± 0.05 eV. This result evidences a secondary phenomenon occurring with prolonged time of sintering, which is deleterious for the electrical conductivity.

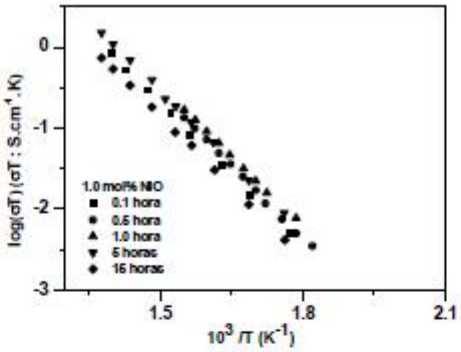

Figure 8. Arrhenius plots of the grain boundary conductivity for 8YSZ containing 1.0 mol% NiO sintered at 1350°C for varying sintering times.

Figure 9 shows a SEM micrograph of 8YSZ with 1.0 mol% NiO after sintering at 1350°C for 15 h. Microstructural defects were generated in specimens exposed to high temperature for long sintering times. This microstructural effect is expected to degrade de mechanical properties of the solid electrolyte as well. These defects are related to some reaction of nickel oxide at high temperature. A careful EDS analysis was carried out in several specimens with varying NiO contents. Figure 10 shows, as an example, one of these plots obtained for 1.0 mol% NiO containing 8YSZ specimen.

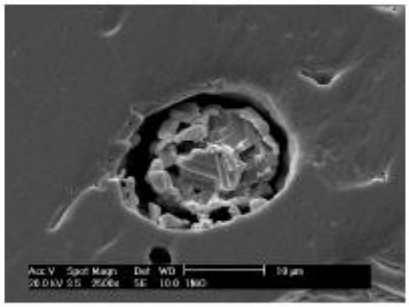

Figure 9. SEM micrograph of 8YSZ with 1.0 mol% NiO. Sintering conditions: 1350°C for 15 h.

In the micro-region containing small grains (center region of figure 9), few of them exhibit a relatively high content of Ni, while keeping constant the relative amounts of Zr and Y. This means that Ni segregated during sintering. This secondary phenomenon may occur on a large scale in Ni-based anode materials. In a previous study on anode degradation it was shown that about 1 wt.% of Ni was found at the interface between the

electrolyte and the Ni-based electrode, whereas regions away from the interface were free of Ni (13). In this study, Ni segregation was found even for specimens containing only 0.5 mol% NiO, that is, below the solubility limit of nickel oxide in the zirconia matrix. Then, special attention should be taken in long-term operation at high temperatures due to possible degradation effects due to Ni segregation. In contrast, for applications at low temperatures, the addition of small amounts of NiO to 8YSZ may be beneficial for improving densification.

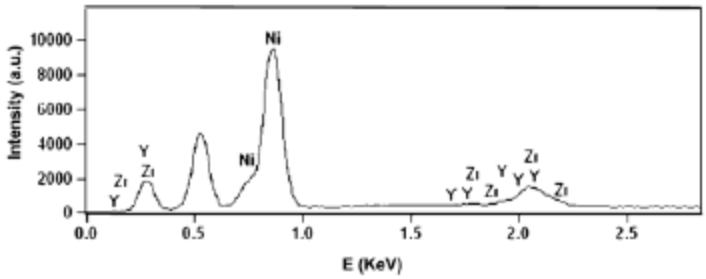

Figure 10. Energy dispersive spectroscopy of 8YSZ with 1.0 mol% NiO sintered at 1350°C for 15 h.

Conclusions

The effect of sintering time on the electrical conductivity of conventionally sintered 8YSZ containing small amounts of NiO was systematically investigated. No differences were observed in the grain conductivity when NiO was used as sintering aid. The apparent activation energy determined by impedance was 1.14 and 1.17 eV for grain and grain boundary, respectively. A significant blocking effect of charge carriers at grain boundaries was found with increasing holding times at 1350°C simultaneously with creation of microstructure defects, due to Ni segregation.

Acknowledgments

The authors acknowledge FAPESP, CNPq and CNEN for sponsoring the facilities used in this work. R. M. B. acknowledges FAPESP for the scholarship.

References

1. S. C. Singhal, *Solid State Ionics*, **135**, 305 (2000).
2. J. W. Fergus, *J. Power Sources*, **162**, 30 (2006).
3. K. C. Radford and R. J. Bratton, *J. Mater. Sci.*, **14**, 66 (1979).
4. M. J. Verkerk, A. J. A. Winnubst and A. J. Burggraaf, *J. Mater. Sci.*, **17**, 3113 (1982).

5. C. Bowen, S. Ramesh, C. Gill and S. Lawson, *J. Mater. Sci*., **33**, 5103 (1998).
6. G. C. T. Silva and E. N. S. Muccillo, *Solid State Ionics*, **180**, 835 (2009).
7. R. C. Weast, CRC *Handbook of Chemistry and Physics*, 64th ed., CRC Press Inc., Florida, USA (1983).
8. J. van Herle and R. Vasquez, *J. Eur. Ceram. Soc*., **24**, 1177 (2004).
9. T. S. Zhang, Z. H. Du, S. Li, L. B. Kong, X. C. Song, J. Lu and J. Ma, *Solid State Ionics*, **180**, 1311 (2009).
10. S. Linderoth, N. Bonanos, K.V. Jensen and J. B. Bilde-Sorensen, *J. Am. Ceram. Soc*., **84**, 2652 (2001).
11. W. G. Coors, J. R. O'Brien and J. T. White, *Solid State Ionics*, **180**, 246 (2009).
12. R. M. Batista and E. N. S. Muccillo, *Ceram. Int*., Doi: 10.1016/ j.ceramint.2010.11.031.
13. Y. L. Liu, S. Primdahl and M. Mogensen. *Solid State Ionics*, **161**, 1 (2001).